

X-ray diffraction study of the structure and thermal parameters of the ternary Au–Ag–Pd alloys

A.B. Ziya^{a,b,*}, K. Ohshima^b

^a Department of Physics, Bahauddin Zakariya University, Multan-60800, Pakistan

^b Institute of Materials Science, University of Tsukuba, Tsukuba 305-8573, Japan

Received 10 October 2005; received in revised form 3 January 2006; accepted 4 January 2006

Available online 14 February 2006

Abstract

In situ X-ray diffraction experiments were performed on six samples of the ternary Au–Ag–Pd alloys (with Al structure) having different compositions using a Cu-target. The integrated intensity data obtained in the temperature range of 373–1200 K was utilized to determine the lattice parameters and the thermal parameters like Einstein's temperatures (Θ_E), the mean-square amplitudes ($\overline{u^2}(T)$) and the coefficients of thermal expansion with a high accuracy. The lattice parameter showed a small negative deviation from the Vegard's rule. It is also found that the mean-square amplitudes are independent of the static displacements. The mean-square amplitudes of vibration and the linear thermal expansion follow the classical Grüneisen relationship in these alloys.

© 2006 Elsevier B.V. All rights reserved.

Keywords: Alloys; Structure; Thermal properties; X-ray diffraction

1. Introduction

The Au(Ag)-based multicomponent alloys have been investigated for use in various technological applications, e.g. biomedical applications, electrical contacts and jewellery, etc. [1]. They are considered suitable for such applications in industry owing to their low electrical resistivity, relatively non-toxic nature and corrosion resistance. Pd is a whitening agent and a significant constituent of the Pd-white golds based on these noble metals. The binary Au–Ag, Au–Pd and Ag–Pd alloys form a continuous series of solid solutions over a wide range of composition and temperature. The ternary alloys of Au, Ag and Pd are thus expected to form single phase solid solutions at all temperatures below the solidus [2].

Since various properties of these alloys depend on the microstructural conditions, the information obtained on their structure and thermal properties can, therefore, be used to design alloys and heat treatments based on such knowledge. One of the important tasks in crystallography is the determination of

the mean-square amplitudes of vibration because such an accurate knowledge is essential for the understanding of the crystal structures or the refinement of known crystal structures. The expansion and contraction of alloys as a result of temperature change is not only of immense theoretical interest but of fundamental importance in many industrial applications [3]. The effect of this phenomenon on alloy specimens is expressed through a coefficient of linear thermal expansion.¹ The scientific understanding and technological importance of thermal expansion of the alloys has lead to the measurement of this property for various materials [3], e.g. the binary Au–Ag [4], Au–Pd [4–7] and Ag–Pd [4,8–9] alloys, but the experimental data on the ternary Au–Ag–Pd alloys is rather limited [3–4].

Naidu and Houska in the pioneer work, studied the variations of the structure of highly deformed fillings of the Au–Ag–Pd alloys in order to explain the hardening mechanisms [3–4]. However, they have reported the values of the lattice parameter and the coefficient of thermal expansion on a few composi-

* Corresponding author. Tel.: +92 61 4745263; fax: +92 61 9210068.
E-mail address: amer_ziya@yahoo.com (A.B. Ziya).

¹ Denoted by α and defined as $(\Delta l/l_0)/\Delta T$, where l_0 is the length of the specimen, $\Delta l/l_0$ the relative elongation and ΔT the change in temperature at the reference temperature.

tions only in the temperature range of 80–298 K. Later, the structure and thermal expansion of these alloys was investigated by Venudhar et al. by the use of graphical extrapolation method [10–11]. It was shown that the lattice parameter increased with the temperature but the coefficient of thermal expansion was found to remain constant with temperature for four compositions. The phase diagram of this alloy is based either on these works or on thermodynamic modeling [12]. A detailed study on the structural properties of these alloys appears to have not been undertaken yet. This work is an effort to study the equilibrium structural and thermal properties of these alloys.

In the present work, we have investigated the structure, the lattice parameters, the characteristic Einstein temperatures, the mean-square amplitudes of vibration and the thermal expansion, of these alloys over a wide range of composition and temperature using the in situ X-ray diffraction technique. In order to demonstrate the effect of alloy composition, six samples, i.e. Au₄₀Ag₄₀Pd₂₀, Au₂₅Ag₂₅Pd₅₀, Au_{33.3}Ag_{33.3}Pd_{33.3}, Au₅₀Ag₂₅Pd₂₅, Au₂₀Ag₄₀Pd₄₀, Au₄₀Ag₂₀Pd₄₀, (hereafter referred to as AAP221, AAP112, AAP111, AAP211, AAP122 and AAP212, respectively) were selected for this work. The composition and temperature dependence of these parameters has been examined and finally the results have been discussed by comparing with those given in literature.

2. Experimental

Round shaped master ingots (~10 gm each) of the polycrystalline AAP221, AAP112, AAP111, AAP211, AAP122 and AAP212 alloys were prepared by conventional arc-melting under an atmosphere of Argon at about 300 Torr pressure, from spectroscopically pure materials and by casting on a copper hearth. Each alloy was remelted 10–12 times to ensure the homogeneity of the relative concentrations of the three types of atoms. No weight losses were recorded and the chemical compositions determined by electron probe microanalysis (EPMA) were nearly the same as the starting compositions. The microanalysis also revealed that the homogeneity variation of the alloys was <1 at.%. Thin slices were cut from the alloy pellets, surface ground and polished to produce a mirror surface suitable for the X-ray diffraction work. The in situ X-ray diffraction experiments were performed with the two circle diffractometer (Philips X'Pert Pro) equipped with a vacuum heating stage (Anton-Paar HTK-16). The diffraction experiments were performed in the step scan mode using Cu K α radiation with θ - θ geometry, Ni-filter, divergence slit 0.5°, receiving slit 0.5° and solid state detector (rapid counting X'Pert X'celerator system). The working conditions were 45 KV and 40 mA for the X-ray tube, scan speed 0.01°/s, a counting time of 10 s per step and angular range from 20 to 130°. The heating unit consisted of vacuum heating chamber with a Pt heater, temperature controller to an accuracy of ± 1 K and Pt-PtRh 10% thermocouple to monitor the temperature of the sample during the measurements. A vacuum level of nearly 7.5×10^{-6} Torr was maintained in the chamber using a turbo molecular pump throughout the measurements.

3. Results and evaluation

3.1. Lattice parameters

The polycrystalline specimens (grain size 40–50 μm) sealed in quartz tubes under a vacuum better than 10^{-6} Torr, were annealed at 1373 K for two weeks and furnace cooled to remove the strains and homogenize them. X-ray diffraction patterns were taken at room temperature (298 K) for all samples. The diffrac-

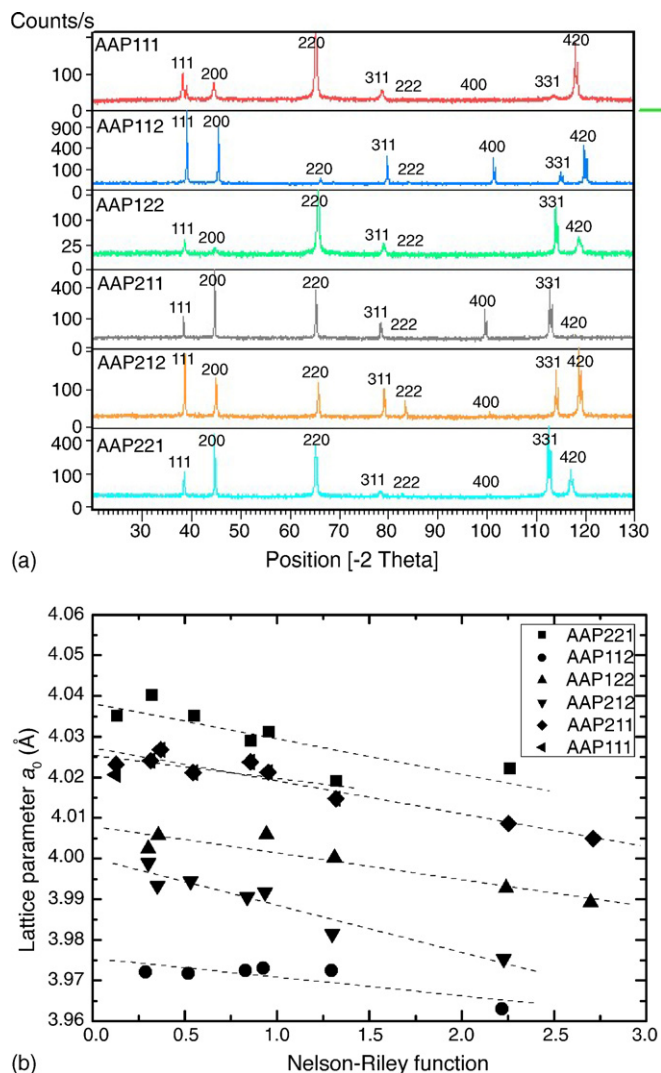


Fig. 1. (a) X-ray diffraction patterns of the Au–Ag–Pd alloys. (b) Room temperature lattice parameters of the Au–Ag–Pd alloys obtained from the Nelson–Riley plot.

tion patterns established that the alloys were single phase with fcc (A1) structure.

Fig. 1(a) shows the diffraction patterns of the six samples. All the expected A1 reflections with $(h^2 + k^2 + l^2) \leq 20$ were seen in the diffraction patterns with K α_1 and the K α_2 lines well separated at high angles. It was possible to deconvolute the lower angle lines so that the Bragg angles for the K α_1 and the K α_2 lines could be determined accurately. The small extra peak near the 111 reflection of the AAP111 sample originates from the Pt heater.

The instrumental errors were corrected by the use of 4N-grade pure silicon as an external standard. The method of least squares fitting of the Nelson–Riley function was used to determine the lattice parameters of the six samples in order to correct the data for the sample dependence and random errors. The results are shown in Table 1. A Nelson–Riley plot of all six samples considered together is shown in Fig. 1(b), where the data shown corresponds to the K α_1 wavelength only.

Table 1
Lattice parameters of the Au–Ag–Pd alloys at 298 K

Sample	a_0 (Å) (Expt.)	a_0 (Å) (Vegard's rule)
AAP221	4.038 ± 0.003	4.046
AAP211	4.027 ± 0.001	4.035
AAP111	4.025 ± 0.002	4.016
AAP122	4.008 ± 0.002	4.008
AAP212	4.000 ± 0.002	4.006
AAP112	3.975 ± 0.002	3.987

3.2. Thermal parameters

3.2.1. The Einstein temperatures and the mean-square amplitudes of vibration

The Einstein temperatures were determined by considering the structure factor amplitudes F of the fundamental reflections for Au–Ag–Pd alloys (A1 structure), given by:

$$F = 4(c_{\text{Au}}f_{\text{Au}}e^{-M_{\text{Au}}} + c_{\text{Ag}}f_{\text{Ag}}e^{-M_{\text{Ag}}} + c_{\text{Pd}}f_{\text{Pd}}e^{-M_{\text{Pd}}}) \quad (1)$$

where c_{Au} , c_{Ag} , c_{Pd} and f_{Au} , f_{Ag} , f_{Pd} are the atomic fractions and atomic scattering factors ($f=f_0 + \Delta f' + i\Delta f''$, where f_0 is the value found in the tables, $\Delta f'$ and $\Delta f''$ are the real and imaginary parts of the dispersion corrections). $\Delta f'$ and $\Delta f''$ for Au, Ag and Pd for Cu K α radiation were obtained from page 149 of Ref. [13].

$$M_i = B_i \left(\frac{\sin^2 \theta}{\lambda^2} \right), \quad i = \text{Au, Ag or Pd} \quad (2)$$

where B is the temperature parameter, θ the Bragg angle and λ the wavelength of the incident X-rays. If the assumption that an average value for the parameter, $\bar{B}(T)$, described by:

$$\bar{B}(T) = B_{\text{Au}}(T) = B_{\text{Ag}}(T) = B_{\text{Pd}}(T) \quad (3)$$

is justified, then the integrated intensity I_{hkl} for the $\{hkl\}$ reflections for a polycrystalline diffractometer sample is given as:

$$I_{hkl} = Kp|F|^2\phi(\theta)e^{-2\bar{M}}, \quad (4)$$

where K is a scale factor, p the multiplicity factor and $\phi(\theta)$ is the Lorentz-polarization factor. Eq. (4) can be rewritten as:

$$I'_{hkl} = \frac{I_{hkl}}{p|F|^2\phi(\theta)} = K(e)^{-2\bar{M}} = K \exp \left(\frac{-2\bar{B}(T) \sin^2 \theta}{\lambda^2} \right) \quad (5)$$

The Einstein's high temperature approximation gives the following equation:

$$\bar{B}(T) = 8\pi^2 \bar{u}^2(T) = \left(\frac{6h^2}{mk_B} \right) \left(\frac{T}{\Theta_E^2} \right), \quad (6)$$

where $\bar{u}^2(T)$ is the mean-square amplitude of the vibrating atom in a direction normal to the diffracting planes, h the Planck's constant, T the absolute temperature, $m=A/N$, the mass of the vibrating atom (where A =atomic weight and N =Avogadro's number), k_B Boltzmann's constant and Θ_E the characteristic Einstein temperature of the alloy in K.

There are two ways to determine the \bar{B} -parameters. One is to use all the hkl intensity data at a fixed temperature. The

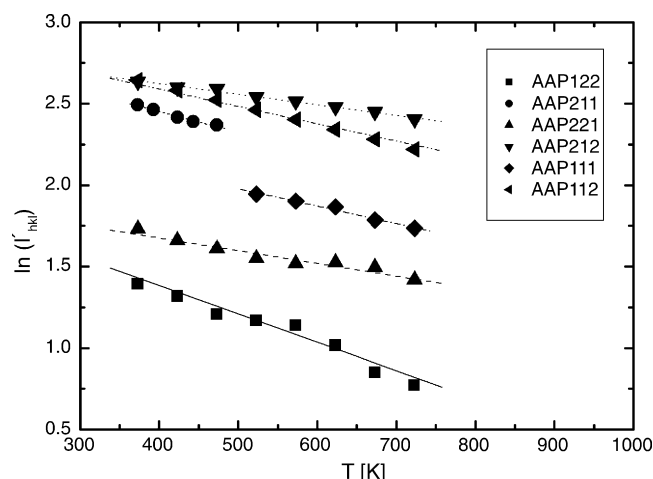


Fig. 2. The plot of $\ln(I'_{hkl})$ versus T for the Au–Ag–Pd alloys. The solid symbols and lines represent the experimental and the least squares fitted data, respectively.

other is to use the temperature dependence of the fixed (hkl) integrated intensity in order to eliminate the effects of preferred orientation. In this analysis, the later has been used as it is more reliable.

Fig. 2 shows the plot of $\ln(I'_{hkl})$ versus temperature (T) for the six samples. It is seen that all points lie near the fitted lines. The intensity data beyond 493 K for AAP211 and below 493 K for AAP111 was not considered because it was scattered. The integrated intensities of the various Bragg reflections were determined by the use of line profile fit software. The integrated intensity of a Bragg reflection was calculated after stripping off the K α_2 -component from the peak intensity and correcting the data for the background. The data shown corresponds to temperatures up to 723 K only because the intensity data beyond this temperature was not linear due to the limitation of the harmonic approximation. Further, the intensity data for only high angle Bragg reflections, e.g. 331, 420, was considered because the intensity of the low angle reflections was found to be nearly independent of temperature. Θ_E was determined from the slope of the $\ln(I'_{hkl})$ versus T plots. $\bar{u}^2(T)$ was estimated from Eq. (6) for various temperatures. The values of the parameters obtained are given in Table 2. The values of the Θ_E and $\bar{u}^2(T)$ are accurate nearly up to $\pm 5\%$ which is within the range of the experimental accuracy.

3.2.2. Thermal expansion

The temperature dependence of the lattice parameter, mean lattice thermal expansion (MLTE)² and coefficient of thermal expansion ($\alpha(T)$)³ between 373 and 1200 K is shown in Fig. 3. The data was corrected for the instrumental, sample dependence and random errors as described earlier. The variations in the lattice parameters could be easily resolved for a temperature step of 10 K which enabled a highly accurate determination

² MLTE(%) = $100 \times [(a(T) - a_{373})/a_{373}]$.

³ $\alpha(T)(K^{-1}) = (1/a(T))(da(T)/dT)$.

Table 2

The characteristic Einstein temperatures (Θ_E) and the mean-square amplitudes ($\overline{u^2}(T)$) of the Au–Ag–Pd alloys

Thermal parameters	Θ_E (K)	Sample					
		AAP122	AAP211	AAP221	AAP212	AAP111	AAP112
		183 ± 6	184 ± 4	248 ± 6	267 ± 6	274 ± 9	305 ± 13
$\overline{u^2}(T)(\text{\AA}^2)$	373	0.0129	0.0105	0.0062	0.0053	0.0053	0.0045
	393	0.0136	0.0111	0.0065	0.0056	0.0056	0.0047
	423	0.0146	0.0119	0.0070	0.0060	0.0061	0.0051
	443	0.0153	0.0125	0.0073	0.0063	0.0063	0.0053
	473	0.0163	0.0133	0.0078	0.0067	0.0068	0.0057
	493	0.0171	0.0139	0.0082	0.0070	0.0071	0.0059
	523	0.0181	0.0147	0.0087	0.0074	0.0075	0.0063
	563	0.0195	0.0159	0.0094	0.0080	0.0081	0.0068
	573	0.0198	–	0.0095	0.0082	0.0082	0.0069
	623	0.0216	–	0.0103	0.0089	0.0089	0.0075
	673	0.0233	–	0.0112	0.0096	0.0096	0.0081
	723	0.0250	–	0.0120	0.0103	0.0104	0.0087

Table 3

The constants A , B , C and D obtained from the temperature dependence of the lattice parameters along with the coefficients of thermal expansion

Sample	$\alpha(373\text{ K})\text{--}\alpha(1200\text{ K}) (\times 10^{-6}) (\text{K}^{-1})$	$A (\text{\AA})$	$B (\times 10^{-5}) (\text{\AA K}^{-1})$	$C (\times 10^{-8}) (\text{\AA K}^{-2})$	$D (\times 10^{-11}) (\text{\AA K}^{-3})$
AAP112	8.19–5.64	3.97	2.52	1.66	–1.19
AAP212	8.68–16.72	3.99	4.75	–3.11	2.51
AAP211	7.62–31.47	4.02	3.76	–3.16	4.00
AAP122	9.84–25.11	3.99	5.35	–3.73	3.29
AAP221	9.07–20.68	4.03	3.03	–0.11	1.73
AAP111	9.66–11.84	4.00	4.67	–1.65	1.06

of $\alpha(T)$. The values of MLTE and $\alpha(T)$ were determined from the lattice parameter using the Bragg line displacement method. The changes in the lattice parameter caused by thermal expansion were calculated from the variations in the positions of the high angle Bragg peaks recorded at various temperatures. Precise determination of the peak positions was made by means of software for powder diffraction analysis. The lattice parameters

for the six samples varied between nearly 3.980 Å and 4.090 Å in the investigated temperature range. $\alpha(T)$ was determined by least squares fitting of the lattice parameter data to a third degree polynomial:

$$a(T) = A + BT + CT^2 + DT^3 \quad (7)$$

The constant B is the coefficient of the linear term and C , D , represent the coefficients of non-linear terms. The values of these constants are listed in Table 3 below.

4. Discussion

The values of the lattice parameters obtained in this work are consistent with those reported by Pearson [14] and Naidu and Houska [4] for these alloys. The data shows a strong dependence of the lattice parameters on the alloy composition and a negative deviation from the Vegard's rule. This observation is in accordance with the expectations as the atomic radius of the Pd-atom is nearly 4% smaller than that of both Au and Ag and its addition is expected to reduce the value of lattice parameter. The lattice parameter of all samples was found to increase with the temperature. The variations in the lattice parameter of AAP111 were smaller than those for the other five alloys.

The experimentally determined temperature parameters from polycrystals contain a static component which arises due to disorder caused by the presence of atoms of different sizes

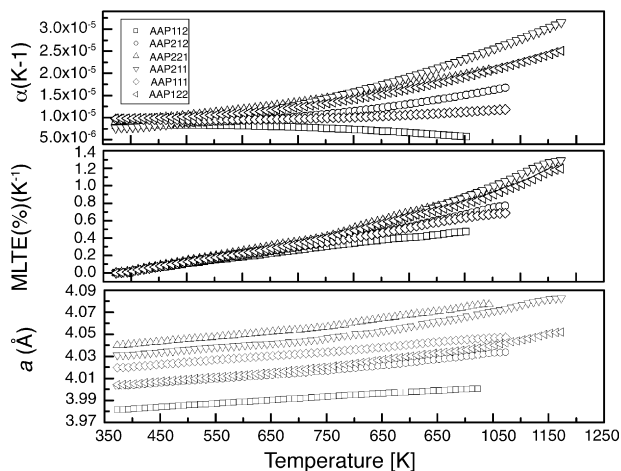


Fig. 3. Temperature dependence of the lattice parameter (a), mean linear thermal expansion (MLTE) and the coefficient of thermal expansion ($\alpha(T)$) of the ternary Au–Ag–Pd alloys.

at lattice points which are normally occupied by a given type of atom, i.e. $\overline{B}(T) = B_{\text{thermal}} + B_{\text{static}}$. This disorder enhances the Debye–Waller factor. The analysis showed that the value of B_{static} for all six samples was nearly zero. Therefore, $\overline{B}(T)$ was assumed equal to B_{thermal} . This is in accordance with the expectations as the atomic sizes of Au, Ag and Pd are nearly similar.

Further, a comparison of the results of AAP221, AAP111 and AAP112 shows that the value of Θ_E increases with the increase of Pd provided at % Au = at % Ag. The same is reflected in the values of $\overline{u^2}(T)$ which should decrease with increase of Pd. Similar results have been reported by Naidu and Houska [4] for Au_{37.5}Ag_{37.5}Pd₂₅, Au₂₅Ag₂₅Pd₅₀ and Au_{12.5}Ag_{12.5}Pd₇₅, although the values reported by them are little scattered. They have found a value of 250 K for the Debye temperature of AAP112 alloy which is slightly different from what the present results yielded. The values of $\overline{u^2}(T)$ found in this work are also slightly different than those reported by Naidu and Houska [4]. The reason for this difference is that their data corresponds to the melting temperatures only.

It was found that the alloy composition has a significant effect on the thermal expansion as well. The total change in $\alpha(T)$ between 373 and 1200 K was found to be –31.14%, 92.63%, 312.99%, 155.18%, 128.0% and 22.56% for AAP112, AAP212, AAP211, AAP122, AAP221 and AAP111, respectively. Below 600 K, the variation of $\alpha(T)$ is nearly similar for all samples. The thermal expansion in this range can be attributed to the electronic and lattice contributions only, but, the electronic contribution can be assumed to be extremely small taking into consideration the investigated temperature range. Above 600 K, the data is non-linear for nearly all the samples the reason for which is the limitation of the harmonic approximation.

The constant A in Eq. (7) represents the lattice parameter of the alloy at absolute zero which corresponds to the zero point motion. $\alpha(T)$ was found to increase with temperature for all samples except AAP112. This is contrary to the observations made by Venudhar et al. [10–11] and is due to the different scheme of thermal treatment used in that work. The decrease in $\alpha(T)$ with temperature observed in the case of AAP112 can be explained if the contributions from linear and non-linear terms are considered. The constants C and D have opposite signs for this alloy as compared to their values for the other five samples. The contribution from the last two non-linear terms in Eq. (7) is quite significant in the case of AAP112. $\alpha(T)$ therefore decreases at high temperatures for this alloy. In general, non-linearity in these alloys depends upon the alloy composition but it was found to be slightly larger in the case of Au or Pd rich alloys. Naidu and Houska [4] have reported a value of 12.7×10^{-6} for $\alpha(80\text{--}298\text{ K})$ for AAP112. A value of 8.19×10^{-6} to 5.64×10^{-6} for $\alpha(373\text{--}1200\text{ K})$ has been obtained for the same alloy in the present work. The agreement between the two is reasonably good keeping in view of the temperature ranges investigated in these studies.

Houska and Stein have shown that the linear thermal expansion of cubic materials is directly proportional to the mean-square amplitude of vibration [15]. The linear thermal expansion

for ternary Au–Ag–Pd alloys⁴ is given by:

$$\frac{(a(T) - a_0)}{a_0} = \frac{(1.47 \overline{u^2}(T))}{v} \quad (8)$$

The plot of MLTE in Fig. 3 demonstrates this relationship for all the investigated alloys.

It can be seen that the values of $\overline{u^2}(T)$ and the MLTE decrease with the increase of Pd. The results suggest that strengthening of the cohesive forces occur as large Au and Ag atoms are substituted by nearly 4% smaller Pd atoms. The present results are in agreement with the previous studies.

5. Conclusions

In situ X-ray diffraction was employed to study the structure and thermal properties of the Au–Ag–Pd alloys. The analysis of the data lead to the determination of the structure, lattice parameters, the characteristic Einstein temperatures, the mean-square amplitudes of vibration and the coefficients of thermal expansion. It is found that both the lattice parameters and thermal parameters depend strongly on the alloy composition. Further, the lattice parameters showed a negative deviation from the Vegard's rule. It is also found that the mean-square amplitudes are independent of the static displacements for all the six alloys. The mean-square amplitudes of vibration and the thermal expansion of were found to obey the classical Grüneisen relationship.

Acknowledgement

One of the authors (A.B.Z.) is grateful to the Higher Education Commission (HEC), Government of Pakistan, for financial support during his stay at the Institute of Materials Science, University of Tsukuba, Tsukuba, Japan, under post doctoral fellowship program—Phase-II, 2003.

References

- [1] A.B. Ziya, T. Abbas, Mater. Chem. Phys. 91 (2–3) (2005) 442–446.
- [2] A.B. Ziya, J. Appl. Crystallogr. 38 (2005) 346–352.
- [3] Y.S. Tolokian, R.K. Kirby, R.E. Taylor, P.D. Desai, Thermal Expansion—Metallic Elements and Alloys, IFI/Plenum Data Company, New York, 1975;
S. Sumithra, A.K. Tyagi, A.M. Umarji, Mater. Sci. Eng. B 116 (2005) 14;
S. Al-Heniti, A. Al-Hajry, J. Alloys Compd. 387 (2005) L5;
J.W. Taylor, H. Capellmann, K.-U. Neumann, K.R.A. Ziebeck, Eur. Phys. J. B 16 (2000) 233.
- [4] S.V.N. Naidu, C.R. Houska, J. Appl. Phys. 42 (12) (1971) 4971.
- [5] H. Masumoto, S. Sawaya, Nippon Kin. Gakk 33 (1) (1969) 121.
- [6] P.L. Spedding, J. Less Common Met. 7 (1964) 395.
- [7] U. Devi, C.N. Rao, K.K. Rao, Acta Metall. 13 (1) (1965) 44.
- [8] A.C. Batley, N. Waterhouse, B. Yates, J. Phys. C: Solid State Phys. 2 (5) (1969) 769.
- [9] C.N. Rao, K.K. Rao, Can. J. Phys. 42 (7) (1964) 1336.

⁴ $\frac{(a(T)-a_0)}{a_0} = \frac{(8\pi^2\gamma Z^2\overline{u^2}(T))}{9v}$, where v is the atomic volume, γ the Grüneisen constant, Z a constant which can be determined from the central force model [16]. $a(T)$ and a_0 have their usual meanings. The value of γZ^2 for ternary Au–Ag–Pd alloys is 0.167 [4].

- [10] Y.C. Venudhar, T.R. Prasad, L. Iyengar, K.V. Krishna Rao, J. Less Common Met. 66 (2) (1979) 11.
- [11] Y.C. Venudhar, L. Iyengar, K.V. Krishna Rao, J. Less Common Met. 60 (2) (1978) 55.
- [12] P. Villars, A. Prince, H. Okamoto, Handbook of Ternary Alloy Phase Diagrams, ASM International, Materials Park, Ohio, 1997.
- [13] J.A. Ibers, W.C. Hamilton, International Tables for X-ray Crystallography, vol. IV, Kynoch Press, Birmingham, 1974.
- [14] W.B. Pearson, A Handbook of Lattice Spacings and Structure of Metals, Pergamon Press, London, 1958.
- [15] C.R. Houska, B.A. Stein, Acta Crystallogr. 21 (1966) 611.
- [16] E. Grüneisen, Handbuch der Physik, Julius Springer, Berlin, 1926.